The simulated H-plane radiation pattern is shown in Fig. 5. The 3-dB beamwidth in the H-plane of ATLSA-P, ALTSA-C and ALTSA-DL is observed to be 29.5°, 33.1° and 25.2° respectively. Further, the side lobe level of ALTSA-P, ALTSA-C and ALTSA-DL in H-plane is observed to be -13 dB, -12 dB and -15dB respectively. Also, the cross polarization level of ALTSA-P, ALTSA-C and ALTSA-DL is seen to be better than 14 dB, 21 dB and 22 dB respectively. It is noted that, though with corrugation the E-plane beamwidth decreases but the beamwidth increases in H-plane. Overall it is found that ALTSA-DL has the narrowest beamwidth, lowest side lobe level and better cross polarization in both E- and H-planes. Therefore ALTSA-DL is found to have the best performance. Hence, ALTSA-DL is fabricated and its performance parameters are measured to validate the design.

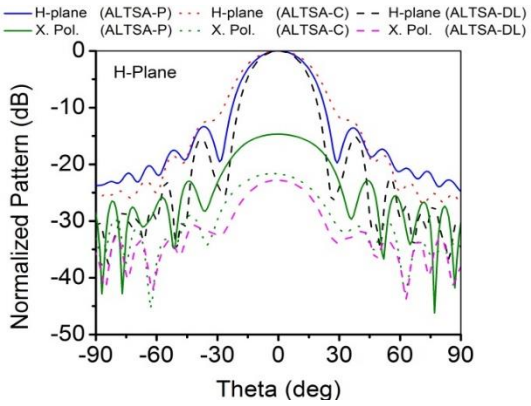

Fig. 5. Simulated H-plane radiation pattern at 60 GHz.

Figure 6 shows the fabricated ALTSA-DL prototype. The dimension of ALTSA-DL is 67.5 mm x 10.1 mm. It is compact in size and light weight. It is fabricated using the low cost printed circuit board (PCB) technology. The S11 parameters and gain of ALTSA-DL are measured utilizing MVNA-8-350 with probe station. The radiation pattern measurement has been performed in a far-field anechoic chamber.

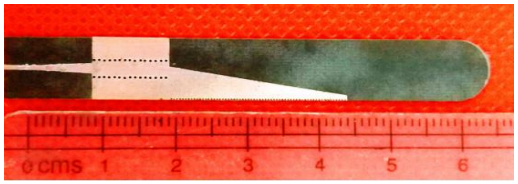

Fig. 6. Fabricated ALTSA-DL.

Figure 7 shows the measured gain and return loss of the ALTSA-DL. From Fig. 7, it is observed that measured gain of ALTSA-DL is 18.7± 0.5 dB over the entire 60 GHz band (57-64 GHz). The antenna gain is almost flat over the entire bandwidth. Similarly, measured return loss is observed to be better than 12 dB over the 60 GHz band. At 60 GHz, return loss is better than 22 dB. The discrepancy observed in the measured return loss with slight frequency shift can be attributed to the fabrication tolerances. Figure 8 shows the measured E-plane radiation pattern of ALTSA-DL at 60 GHz. The measured 3-dB beamwidth of ALTSA-DL in E-plane is 17° and the side lobe level is at -17 dB, which is similar to the values obtained from simulation. Similarly, Fig. 9 shows the measured H-plane radiation pattern of ALTSA-DL at 60 GHz. The measured 3-dB beamwidth of ALTSA-DL in H-plane is observed to be 22.7° and the side lobe level is at -15.7 dB. Further, it is seen that the simulated and measured radiation patterns are in good agreement in both E-plane and H-plane. Also, the radiation efficiency is observed to be 92%.

Table 1 lists the comparison with other SIW based antennas having different dielectric loading structures such as rectangle in [6], elliptical in [8] etc. It is observed that though the proposed antenna has less impedance bandwidth as compared to [7], its gain is better as compared to other antennas. Further, its impedance bandwidth covers 57-64 GHz, which is adequate for multi-Gbps communication at 60 GHz.

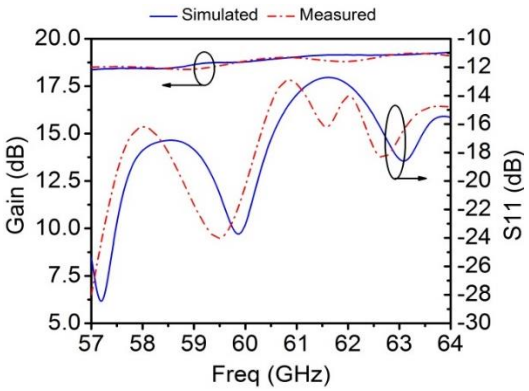

Fig. 7. Simulated and measured return loss and gain of ALTSA-DL.

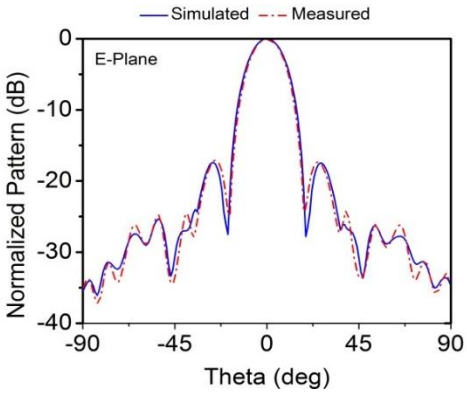

Fig. 8. Simulated and measured E-plane radiation pattern of ALTSA-DL at 60 GHz.

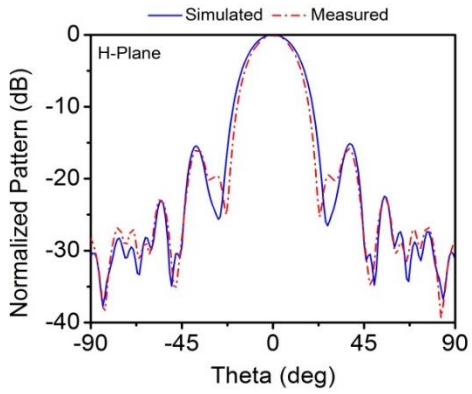

Fig. 9. Simulated and measured H-plane radiation pattern of ALTSA-DL at 60 GHz.

Table 1: Comparison with other antennas

Parameter	[6]	[7]	[8]	This Work
Antenna	Horn	ALTSA	ETSA	ALTSA
Dielectric loading structure	Rect.	Diamond slot	Ellip.	Rect. with semicircular top
Gain (dBi)	9.7	16.2	11.4	18.8
Impedance bandwidth	5.5%	33.3%	5.5%	11.6%
Operation frequency (GHz)	27	60	60	60

IV. CONCLUSION

A high gain ALTSA with dielectric loading is presented in this paper. The antenna has high gain, compact size, light weight, ease of fabrication using PCB technology and it is also fit for mass production. Hence, the proposed antenna is suitable for high speed communication in 60 GHz band.

ACKNOWLEDGMENT

Authors are very much obliged to ISRO, Government of India, for their assistance provided for the execution of this research work.

REFERENCES

[1] P. Smulders, "Exploiting the 60 GHz band for local wireless multimedia access: Prospects and future directions," *IEEE Communication Magazine*, vol. 40, pp. 140-147, 2002.

[2] M. Bozzi, A. Georgiadis, and K. Wu, "Review of substrate-integrated waveguide circuits and antennas," *IET Microwaves, Antennas & Propagation*, vol. 5, pp. 909-920, 2011.

[3] T. Djerafi and K. Wu, "Corrugated substrate integrated waveguide antipodal linearly tapered slot antenna array fed by quasi-triangular power divider," *PIER C*, vol. 26, pp. 139-151, 2012.

[4] P. Shrivastava, D. Chandra, N. Tiwari, and T. R. Rao, "Investigations on corrugation issues in SIW based antipodal linear tapered slot antenna for wireless networks at 60 GHz," *ACES Journal*, vol. 28, pp. 960-967, 2013.

[5] N. Ghassemi and K. Wu, "Planar high-gain dielectric-loaded antipodal linearly tapered slot antenna for E- and W-band gigabyte point-to-point wireless services," *IEEE Transactions on Antennas and Propagation*, vol. 61, pp. 1747-1755, 2013.

[6] H. Wang, D. G. Fang, B. Zhang, and W. Q. Che, "Dielectric loaded substrate integrated waveguide (SIW) H-plane horn antennas," *IEEE Transactions on Antennas and Propagation*, vol. 58, pp. 640-647, 2010.

[7] I. Mohamed and A. Sebak, "Dielectric loaded antipodal linearly tapered slot antenna for 60 GHz applications," *Global Symposium on Millimeter Waves*, pp. 1-2, 2015.

[8] S. Ramesh and T. R. Rao, "Planar high gain dielectric loaded exponentially tapered slot antenna for millimeter wave wireless communications," *Wireless Personal Communications*, vol. 84, pp. 3179-3192, 2015.